RSC Advances

This is an *Accepted Manuscript*, which has been through the Royal Society of Chemistry peer review process and has been accepted for publication.

Accepted Manuscripts are published online shortly after acceptance, before technical editing, formatting and proof reading. Using this free service, authors can make their results available to the community, in citable form, before we publish the edited article. This *Accepted Manuscript* will be replaced by the edited, formatted and paginated article as soon as this is available.

You can find more information about *Accepted Manuscripts* in the Information for Authors.

Please note that technical editing may introduce minor changes to the text and/or graphics, which may alter content. The journal's standard Terms & Conditions and the Ethical guidelines still apply. In no event shall the Royal Society of Chemistry be held responsible for any errors or omissions in this *Accepted Manuscript* or any consequences arising from the use of any information it contains.

ROYAL SOCIETY OF CHEMISTRY

www.rsc.org/advances

Thyroid-Stimulating Hormone (TSH)-armed Polymer-Lipid Nanoparticles for the Targeted Delivery of Cisplatin in Thyroid Cancers: Therapeutic Efficacy Evaluation

Xue-jun Gao[1], Ai-qin Li[2], Xin Zhang[1], Ping Liu[3], Jue-Ru Wang[1], Xia Cai[4*]

[1]Department of Thyroid Surgery，Affiliated Hospital of Qingdao University; Qingdao 266000, China
[2]Affiliated Hospital of Qingdao University, Qingdao 266000, China
[3]Department of Pharmacy, Shandong Provincial Hospital Affiliated to Shandong University, Jinan 250021, China
[4]Department of Plastic Surgery，Affiliated Hospital of Qingdao University; Qingdao 266000, China

Corresponding author: Xia Cai, M.D
Department of Plastic Surgery，
Affiliated Hospital of Qingdao University, No.111, Jianxi Road, Qingdao 266000, P.R.China
Tel & Fax: 0086-0532-82913018
Email: caixiarty@hotmail.com

RSC Advances Accepted Manuscript

Abstract

Thyroid-stimulating hormone (TSH)-conjugated polymer-lipid hybrid nanoparticle (TPLHC) was developed for the targeted delivery of cisplatin (CDDP) in thyroid cancers. In the present study, polymer-lipid hybrid nanoparticle was conjugated to TSH which will bind to TSH receptor (TSHr) on the surface of thyrocytes. The delivery system was mainly designed to achieve high concentration in thyroid carcinoma. The TPLHC exhibited excellent properties featured by a nanoscaled size of 160 nm with a narrow distribution to benefit EPR-based passive targeting. The polymer-lipid nanoparticle efficiently controlled the release of drug in the physiological conditions. The TSH-conjugated nanoparticles displayed higher cellular uptake in cells which overexpress TSHr. Consistently, TPLHC showed high intracellular levels of CDDP in FTC-133 cancer cells. Specially, TSH-conjugated nanoparticles showed a significantly enhanced anticancer effect than any other groups across all time points and all the concentrations tested. Additionally, 4-fold higher accumulation of TSH-conjugated NP was observed in tumors than compared to non-targeted NP in xenograft mice. Importantly, TPLHC inhibited the growth of tumors more efficiently than compared with other formulations. The enhanced tumor inhibition might be attributed to the specific binding of TSH to the TSHr overexpressed in FTC-133 tumors. Taken together, TSH-conjugated nanoparticles hold great potential to be an effect and safe nanoscale delivery system for the targeted therapy of thyroid cancers.

Keywords

Thyroid cancer, cisplatin, thyroid-stimulating hormone, nanoparticles, thyroid gland

RSC Advances Accepted Manuscript

Introduction

Thyroid cancer is a disease in which malignant cells arise from thyroid gland. Thyroid cancer is a rare type of cancer that affects the thyroid gland [1]. It is most commonly occurred in age groups between 35-40 years and specifically women are more prone to develop thyroid cancer than men. In UK, thyroid cancers account for less than 1% of total cancer cases registered. At present, either surgical removal of thyroid gland or radiotherapy or a combination of surgery and radiotherapy is performed to treat thyroid cancers [2]. Chemotherapy is not very common choice of treatment in case of thyroid cancer, however, it has been reported that if the cancer in the thyroid gland has been detected in the early stages then chemotherapy can be induced. One of the main obstacles in chemotherapy of thyroid gland is the anatomical location of this gland in the body [3,4]. Therefore, a smart approach has to be adopted for the successful delivery of anticancer agent in the specific location.

Cisplatin (CDDP), a potent anticancer drug is often indicated for the treatment of thyroid cancer [5]. CDDP binds to DNA and causes DNA cross linking which triggers cell apoptosis when repair proves unsuccessful. Despite its potent anticancer effect, the therapeutic effect of CDDP has been limited due to serious side effects such as nephrological and neurological toxicities [6,7]. Nephrotoxicity is a major cause of CDDP associated acute and chronic morbidity, while neurotoxicity is cumulative-dose dependent. Despite the associated side effects, one of the major concerns is the rapid inactivation of the drug through non-specific protein binding in the blood stream, resulting in less therapeutic efficacy and undesirable side effects [8,9]. With regard to thyroid cancer, CDDP will be effective if it can be delivered directly in to the thyroid tissue. As the administration of CDDP directly to the thyroid is difficult, intravenous administration is preferred wherein drug will accumulate in the cancers over a period of time. One of the potential

RSC Advances Accepted Manuscript

disadvantages of IV administration is the rapid inactivation of free drugs in the systemic circulation. Therefore, a novel concept revolving around increasing the therapeutic window, increasing the therapeutic efficacy, and reducing the side effects should be adopted.

In this regard, use of biodegradable polymeric nanoparticles such as poly(lactic-co-glycolic acid) PLGA NP is gaining increasing importance owing to its excellent features such as high loading capacity and controlled drug release pattern [10,11]. In particular, PEG-substituted polymers offer stearic protection to the carrier system in the systemic circulation [12]. However, polymeric NP often shows limited systemic stability and circulation half-lives [13]. Therefore, we have combined the benefits of polymer and lipid and made a fusion NP [14]. The fusion NP is a simple and single step based efficient formulation strategy. In this case, PLGA polymeric NP will form the core which is surrounded by a monolayer of soybean phosphatidylcholine and 1,2-distearoylsn-glycero-3-phosphoethanolamine-N carboxy(polyethylene glycol)2000. Especially, PEG shell provides electrostatic and steric stabilizations and exhibits the longer circulation half-life. In order to increase the specificity to the cancer, active targeting moiety could be attached to the surface of NP [14,15]. For example, antibody fragment against human epidermal growth factor receptor 2 (HER2) which is overexpressed in breast cancer could be tagged to the NP [16, 17]. There are several reports wherein folate residues are attached on the NP surface to increase the selectivity towards folate receptor overexpressed cancer cells. Although there are several antibody tagged nanocarriers, however there is limited study in organ targeted delivery system [18-20]. Especially, there is no report on the targeted drug delivery to thyroid gland.

In this work, we attempted to increase the concentration of anticancer agent in the thyroid gland in order to increase the therapeutic efficacy in thyroid cancer. Towards this goal, we have conjugated thyroid-stimulating hormone (TSH) to the surface of polymer-lipid nanoparticles.

RSC Advances Accepted Manuscript

DSPE-mPEG2000- 3-(2-pyridyldithio)propionate (PDP) was employed to conjugate TSH. The PDP moieties present on the NP surface was reduced by 1,4-dithiothreitol (DTT) to express the free –SH group which was then conjugated with the TSH. The TSH-receptor (TSHr) is a glycoprotein G-protein-coupled receptor which is expressed in the plasma membrane of thyrocytes. The presence of TSH on the NP surface will increase its accumulation in the cancer cells via a ligand-mediated biological effect [21,22]. In vivo accumulation of NP was monitored using animal model and antitumor efficacy was demonstrated.

Result and Discussion

In the present study, TSH-conjugated nanoparticles were prepared to increase the specificity towards the thyroid cancers. TSH was attached to the PDP-conjugated nanoparticle surface via a thiol-activated functional group and forms a disulphide bond (Figure 1). TSH-receptor (TSHr) is a glycoprotein G-protein-coupled receptor which is expressed in the plasma membrane of thyrocytes. The presence of TSH on the NP surface will increase its accumulation in the cancer cells via a ligand-mediated biological effect. In vivo accumulation of NP was monitored using animal model and antitumor efficacy was demonstrated.

Dynamic light scattering analysis

The particle size and size distribution of nanoparticles were observed using dynamic light scattering method (DLS). The average particle size of CDDP-loaded TSH-conjugated polymer-lipid hybrid nanoparticles (TPLHC) was observed to be 185.8 nm with an excellent polydispersity index of 0.12 (Figure 2a). A slight increase in particle size from 152.5 nm to 185.8 for TSH conjugation was attributed to the presence of additional molecular mass from TSH

RSC Advances Accepted Manuscript

itself. Nevertheless, final particle size was less than <200 nm indicating the possibility of passive targeting via a unique enhanced permeability and retention (EPR) effect. The nanoparticle upon long circulation will accumulate in the tumor tissues [23,24]. The TSH conjugation on the nanoparticle surface was further confirmed by the zeta potential evaluation. The surface of bare lipid nanoparticle was -28 mV while it decreased to -19.2 mV for the conjugation of TSH. We have observed that the particle size of TSH-conjugated nanoparticles slightly increased compared to that of non-conjugated nanoparticles. The colloidal stability of TSH-NP was checked for 12h, the particle sizes remained unchanged (DLS analysis). ELISA assay was performed to evaluate the stability of TSH in the biological fluid. For this purpose, TSH was incubated for 3h in growth media supplemented with 10% FBS as well as in phosphate buffered saline (pH 7.4) and acetate buffered saline (pH 5.5). The results revealed that TSH maintains good stability all the tested conditions. Based on the result, it can be expected that TSH surface-conjugated nanoparticle would maintain stability in the in vivo conditions and would be available for the selective targeting of the therapeutic systems.

Particle morphology

TEM was used to investigate the morphology of nanoparticles. As seen, TSH-conjugated nanoparticles were present as an individual spherical object on the copper grid and no sign of aggregation was observed (Figure 2b). A well-defined morphology and spherical shape is expected to increase the systemic performance. A greyish shell on the outer surface a darker core clearly reveals the lipidic shell and polymer core structure. The smaller size of the micelles observed by TEM compared to that determined by DLS was due to the dehydration of the micelles during drying and staining of the TEM specimen.

RSC Advances Accepted Manuscript

Drug loading and Drug release kinetics

Knowledge of drug entrapment efficiency is very important for drug delivery applications. The TPLHC exhibited a high entrapment efficiency of >95% with a high drug loading of ~22.6%. The drug release study was evaluated using dialysis method in phosphate buffered saline (pH 7.4 conditions) at 37°C. The release study was performed in PBS medium in order to simulate the blood environment. As seen (Figure 3), both CDDP-loaded polymer-lipid hybrid nanoparticles (PLHC) and TPLHC exhibited a controlled release profile for 48h. Specially, no burst release phenomenon was observed suggesting that the entire drug was incorporated in the nanoparticle and present in the core of PLGA NP and not present on the lipid shell. As expected, presence of TSH relatively limited the rate of drug release over a period of time. Approximately, 50% of CDDP released from TPLHC compared to that of 65% from PLHC at the end of 24h. Such a low or controlled release of drug in the pH 7.4 conditions was highly advantageous to targeted cancer therapy since the amount of drug released prematurely might be minimized in blood circulation. On the other hand, one could expect that intracellular levels of drug could be increased once internalized via endocytosis.

Intracellular accumulation of nanoparticles

The selectivity of PLHC and TPLHC towards wild-type Chinese hamster ovary (CHO) cells lacking the TSHr (CHOw) and in TSHr overexpressed CHO cells. As seen (Figure 4a-c), wild-type CHO cells which don't express TSHr did not have any influence on the cellular uptake of either nanoparticle. The cellular uptake efficiency of both the nanoparticles was same regardless of presence of TSH on nanoparticles. While the trend was different in case of the CHO-t cells which express the receptor for TSH. The TPLHC exhibited an enhanced cellular uptake on

RSC Advances Accepted Manuscript

CHO-t cells compared to that of PLHC. Simultaneously, competitive binding nature of PLHC and TPLHC towards CHO-t cell was evaluated. As seen, TSH-conjugated nanoparticles showed a decrease in the cellular uptake with the increase in the concentration of TSH in the incubated medium, while, cellular uptake of non-conjugated nanoparticles were independent of TSH level in the medium. All this evidence collectively suggests the preferable interaction of TSH nanoparticle with the receptor expressed cells.

Intracellular uptake of PLHC and TPLHC

The intracellular uptake of cisplatin loaded PLHC and TPLHC in FTC-133 thyroid cancer cell was studied as a function of time. As seen (Figure 5a), intracellular uptake of CDDP significantly increased in the cell group treated with TSH-conjugated NP. Approximately, 10 ng/ml of CDDP was internalized from PLHC compared to that of TPLHC which exhibited a 25 ng/ml at the end of 8h. The results clearly depict the ability of TSH-conjugated nanoparticles as a potent delivery vehicle. The higher cellular uptake was further confirmed by means of confocal imaging. It can be clearly seen that TPLHC exhibited a prominent red fluoresnce compared to that of non-targeted delivery system (Figure 5b) It can be expected that higher intracellular uptake of CDDP would result in greater anticancer effect in cancer cells.

In vitro anticancer effect

Subsequently, anticancer effect of free CDDP, PLHC and TPLHC in FTC-133 thyroid cancer cell was investigated by MTT assay. The cells were incubated for 24, and 48h, respectively and studied the cytotoxic potential individual formulations. As seen, drug-loaded nanoparticles exhibited a significantly higher cytotoxic effect in thyroid cancer cells than compared to free CDDP (Figure 5c-d). Specially, TSH-conjugated nanoparticles showed a significantly enhanced

RSC Advances Accepted Manuscript

anticancer effect than any other groups across all time points and all the concentrations tested. IC50 value was calculated to quantify the effect of individual formulation on the cancer cells. The IC50 value of free CDDP, PLHC and TPLHC were 4.26 µg/ml, 2.31 µg/ml, and 0.52 µg/ml, respectively after 24h incubation. The superior anticancer effect of TPLHC was attributed to the high intracellular concentration of CDDP due to the receptor mediated uptake of nanoparticles in the cancer cells. It is more evident from the fact that uptake of NP decreased when the concentration of TSH was increased in CHO cells. Overall, results suggest that the presence of TSH on the surface of nanoparticle could markedly improve the delivery of drug in the cancer cells expressing TSHr [25,26].

Biodistribution of nanoparticles

The experiments evaluating the distribution of targeted and non-targeted nanoparticles were performed in Wistar rats (Figure 6). For cancer targeting, enhanced accumulation of nanoparticles in the tumor tissue is of great importance. As seen from Figure 3a-c, 4-fold higher accumulation of TSH-conjugated NP was observed than compared to that of non-targeted NP. This could be due the interaction of TSH-NP with the TSHr overexpressed in the thyroid cancer cells. It is worth noting that TPLHC did not accumulate in other organs such as heart, kidney, spleen, and lungs in higher proportion. The biodistribution study therefore clearly depicted the in vivo targeting ability of TPLHC to thyroid glands.

In vivo anticancer efficacy

In vivo anticancer efficacy study of various CDDP formulations were examined in FTC-133-bearing tumor xenograft animal model. The antitumor efficacy of individual formulations was evaluated by measuring the tumor volume at specified time interval to assess the tumor inhibition

RSC Advances Accepted Manuscript

effect. All the mice were alive during the course of entire study period. The growth curves of tumor treated with different formulations are presented in Figure 7a. The blank nanoparticle did not had any effect on the growth of tumors, while all the formulations effectively retarded or delayed the growth of tumor comparing to that of untreated control group. Specially, TPLHC which has TSH conjugated on its surface inhibited tumor growth more efficiently than compared with other mice groups, indicating that targetability and pH-sensitivity could favor increased tumor inhibition [27,28]. The final tumor volumes remained at ~2500 mm^3, ~1600 mm^3, ~1400 mm^3, and ~700 mm^3, respectively for control, free CDDP, PLHC, and TPLHC. The enhanced tumor growth might be attributed to the specific binding of TSH to the TSHr overexpressed in FTC-133 tumors, which facilitate the intracellular uptake through receptor-mediated endocytosis and enhance the suppression effect of CDDP on cancer cell proliferation.

The body weight of mice was monitored throughout the study period which is an important indicator for systemic toxic and side effects. As seen (Figure 7b), none of the formulations induced any loss of body weight implying that free drug as well as delivery system was safe and had good biocompatibility profile. Overall, TPLHC was an effective and safe drug formulation for the treatment of thyroid cancers.

Conclusion

In conclusion, TSH-conjugated polymer-lipid hybrid nanoparticle was successfully developed based on PLGA/DSPE polymer-lipid mixture and TSH conjugation for the treatment of thyroid cancer. The delivery system was mainly designed to target thyroid gland to achieve high concentration in thyroid carcinoma. The TPLHC exhibited excellent properties featured by nanoscaled size of 160 nm with a narrow distribution to benefit EPR effect. The polymer-lipid

RSC Advances Accepted Manuscript

nanoparticle efficiently controlled the release of drug in the physiological conditions. The TSH-conjugated nanoparticles displayed higher cellular uptake in cells which express TSHr. Consistently, TPLHC showed high intracellular levels of CDDP in FTC-133 cancer cells. Specially, TSH-conjugated nanoparticles showed a significantly enhanced anticancer effect than any other groups across all time points and all the concentrations tested. Additionally, 4-fold higher accumulation of TSH-conjugated NP was observed in tumors than compared to non-targeted NP in xenograft mice. Importantly, TPLHC inhibited the growth of tumors more efficiently than compared with other mice groups. The enhanced tumor inhibition might be attributed to the specific binding of TSH to the TSHr overexpressed in FTC-133 tumors. Taken together, TSH-conjugated nanoparticles held great potential to be an effect and safe nanoscale delivery system for the targeted therapy of thyroid cancers.

Materials and Methods

Materials

PLGA (poly(D,L-lactide-co-glycolide), MW~12000) with a 50:50 monomer ratio with viscosity of 0.72-0.92 dl/g and lecithin was purchased from Sigma-Aldrich, China. DSPE–PEG2000 (MW~2790.5) and 1,2-distearoyl-sn-glycero-3-phosphoethanolamine-N-[PDP(methoxypolyethylene glycol-2000)] (DSPE-mPEG2000-PDP (MW~2987.8)) was purchased from Avanti Polar Lipids, China. TSH (from human pituitary), N-(fluorescein-5-tiocarbamoyl)-1,2-dihexadecanoyl-sn-glycero-3-phosphoethanolamine triethylammonium salt (fluorescein-DHPE was purchased from Sigma-Aldrich, China. All other chemicals were of reagent grade.

Preparation of lipid-assembled polymeric nanoparticles

RSC Advances Accepted Manuscript

The fusion nanoparticles were prepared by nanoprecipitation method. Briefly, PLGA was dissolved in dichloromethane at a concentration of 20 mg/ml. Subsequently, lecithin, DSPE-PEG2000, DSPE-mPEG2000-PDP, and cisplatin (CDDP, 10%w/w) was dissolved in 4% ethanol solution and heated to 60°C. The polymer solution was added drop-by-drop on the lipid solution and vortexed. The organic mixtures were stirred for 2h until organic solvents were evaporated. The formed nanoparticles were collected by centrifuging at high speed.

The TSH-conjugated polymer-lipid nanoparticles were prepared by the reduction of disulfide bonds on the surface. For this purpose, NP were treated with 50 mM DTT solution for 30 min. Subsequently, free DTT was removed by centrifugation. The TSH (in nanomolar concentration) was added to the above NP and incubated overnight. The unconjugated TSH was removed by gel permeation chromatography.

Nanoparticle characterization

The particle size of NP was determined by Quasi-elastic laser light scattering using a ZetaPALS dynamic light scattering (DLS) detector (15 mW laser, incident beam = 676 nm) (Brookhaven Instruments, Holtsville, NY). The zeta potential of nanoparticles were determined using Zetasizer ZS Nano (Malvern Instruments, UK).

Transmission electron microscopy

The morphology of NP was observed using JEOL JEM-200CX instrument at an acceleration voltage of 200 kV. 300-mesh carbon-coated copper grid was used to load the samples. The aqueous solution of NP was placed on the TEM grid and blotted away after 20 min. The samples were negatively stained with 2% phosphotungistic acid. The grids were dried and observed under TEM instrument.

RSC Advances Accepted Manuscript

Drug release study

The release profile of CDDP from PLHC and TPLHC was observed in phosphate buffered saline (PBS pH 7.4) at 37°C. For this purpose, 1 ml of nanoparticle dispersion was sealed in a dialysis bag and incubated in 100 ml of PBS. At specified time intervals, 1 ml of release medium was withdrawn and replaced with equal amount of fresh release medium. The amount of CDDP released in the medium was determined by ICP-MS method. A Quadrupole ICP-MS Thermo X-series (Thermo Electron, Windsford, Cheshire, U.K.) equipped with a Meinhard nebulizer, a Fassel torch, and an Impact Bead Quartz spray chamber cooled by a Peltier system was employed for total Pt determination. ICP-MS operating conditions were the following: forward power 1250 W, plasma gas 15 L/min, auxiliary gas 0.73 L/min, nebulizer gas 0.85 L/min, channels per AMU 10, and integration time 0.6 ms.

Cell culture

The selectivity of non-conjugated and TSH-conjugated NP was tested in TSHr expressing CHO cells and CHO wild type cells (without TSHr). The cells were grown on F12 medium containing 10% FBS and 1% penicillin-streptomycin combination. Meanwhile, FTC-133 thyroid cancer cell was incubated in DMEM/F12 (1:1) supplemented with glutamate, D-glucose, pyruvate, and other regular ingredients of normal growth media. The cells were grown in ambient conditions and media was changed and cells were sub-cultured time to time.

Intracellular accumulation of PLHC and TPLHC

RSC Advances Accepted Manuscript

The fluorescent labelled nanoparticles were used to observe the nanoparticle uptake and affinity towards cancer cells and TSHr overexpressed cells. For this study, TSHr non-expressing CHO-w and TSHr expressing CHO-t cells were used. The cells were seeded in a 6-well culture plates and incubated overnight and treated with respective formulations. As a control experiment, free TSH of different concentrations was used to investigate the competitive binding of nanoparticles to the cells. The formulations were incubated for 3h, cells were collected, centrifuged, and media was removed. Cells were then dissolved in quaternary ammonium hydroxide solution and shaken for 1h at 60°C. After incubation for 1h, cells were treated with liquid scintillation cocktail and the samples were vigorously mixed and analyzed using Wallac Win Spectral 1414 liquid scintillation counter.

Intracellular uptake of PLHC and TPLHC

CHO-w and CHO-t cells were seeded in a 12-well culture plate and incubated overnight for the cells to get attached. In brief, cells were exposed with respective formulations and incubated for predetermined time intervals. At specific time intervals, cells were harvested, washed, and resuspended in PBS. The cells were ruptured using a probe sonicator. The ruptured cell suspensions were centrifuged and supernatant was collected. The internalized drugs were present in the supernatant solution. The CDDP signals were determined with Agilent 7700x ICP-MS.

Cytotoxicity assay

MTT assay was performed to evaluate the cytotoxicity potential of free CDDP, PLHC and TPLHC and dose-response curve was plotted. FTC-133 thyroid cancer cell was used in the present study and cell survival was noted after the assay protocols. In brief, 1×10^4 cells were seeded in a 96-well plate in 100 µl of DMEM/F12 medium and incubated for 24h. When the

RSC Advances Accepted Manuscript

cells reached 80% confluence, cells were treated with various concentrations of blank, free CDDP, PLHC and TPLHC formulations and further incubated for 24h, 48h, and 72h, respectively. After each time point, the derivatives in the medium were removed and 20 µl of MTT (5 mg/mL in MEM) was added and incubated for 4 h under normal growing conditions in the incubator. After 4h, 100 µl of DMSO was added and placed for 30 min. After 30 min, optical density (OD) at 570 nm was measured using a plate reader. Cells without polymers were taken as control.

In vivo biodistribution study

The studies on experimental animals were carried out strictly according to the guidance framed by 'Institutional Animal Care and Ethics Committee', Qingdao University, China. All ethics protocols were followed while handling the animals. Female Wistar rats (4-5 months) were selected to perform the biodistribution study. [3H]CHE-radiolabeled PLHC and TPLHC were injected via tail vein into the rats. After 4h, the rats were sacrificed and individual organs were collected. The organs were mixed with quaternary ammonium hydroxide solution and shaken for 1h at 60°C in an incubator shaker. The tissue samples were decolorized with 2 mL of 24% (v/v) H2O2 at room temperature for 1h. After incubation for 1h, cells were treated with liquid scintillation cocktail and the samples were vigorously mixed and analyzed using Wallac Win Spectral 1414 liquid scintillation counter.

Anticancer efficacy study

The anticancer efficacy was studied in NOD SCID mice. FTC-133 cancer cells (1×10^6) cells were subcutaneously injected into the mice and allowed the tumor to grow up to a tumor volume of ~400-500 mm^3. Following which the mice were randomly divided into 5 groups with 8 mice

RSC Advances Accepted Manuscript

in each group. The 5 groups were control, blank NP, free CDDP, PLHC, and TPLHC, respectively. The formulations were injected 3 times into the mice via tail vein at a fixed dose of 5 mg/kg. The tumor volume was measured at specific point of time. The tumor volume was calculated from the equation; $V=0.5\times D\times d^2$, where V is tumor volume, D and d were longest and shortest diameter of the tumor. Body weight of the mice was subsequently monitored on regular basis. The animal experiments were carried out in accordance with the guidelines framed by Affiliated Hospital of Qingdao University, China.

Statistical analysis

The results were statistically analyzed using Student's *t*-test with the level of significance set at $p<0.05$. The significance was tested using GraphPad Prism 5 software (GraphPad Software Inc., USA). The results are expressed as mean±standard deviation.

Acknowledgement

This research was supported by grants from the National Natural Science Foundation of China (No.81171816), and the Science and Technology Research Foundation of Shandong Province (No.2008GG10202045).

References

1. A. Mehta, L. Zhang, M. Boufraqech, Y. Zhang, D. Patel, M. Shen, E. Kebebew, *Endocr Relat Cancer*. 2015, **22**, 319.
2. H. Luo, S. Tulpule, M. Alam, R. Patel, S. Sen, A. Yousif, *Case Rep Oncol*. 2015, **13**, 233.

RSC Advances Accepted Manuscript

3. L. Lorusso, K. Newbold, *Future Oncol*. 2015, **11**, 1719.
4. P. Valderrabano, V.E. Zota, B. McIver, D. Coppola, M.E. Leon, *Cancer Control*. 2015, **22**,152.
5. A. Longhi, C. Errani, M. De Paolis, M. Mercuri, G. Bacci, *Cancer Treat Rev*. 2006, **32**, 423.
6. X. Yanand, R.A. Gemeinhart, *J Control Release*. 2005, *106*, 198–208.
7. E. Cvitkovic, *Cancer Treat Rev*. 1998, **24**, 265–81
8. B.L. van Leeuwen, W.A. Kamps, H.W.B. Jansen, H.J. Hoekstra, *Cancer Treat Rev*. 2000, **26**, 363.
9. S. Sevenson, D.A. Tomalia, *Adv Drug Deliv Rev*. 2005, **57**, 2106.
10. F. Gu, L. Zhang, B.A. Teply, N. Mann, A. Wang, A.F. Radovic-Moreno, et al, *Proc Natl Acad Sci U S A* 2008, **105**, 2586.
11. L. Zhang, A.F. Radovic-Moreno, F. Alexis, F.X. Gu, P.A. Basto, V. Bagalkot, et al, *ChemMedChem* 2007, **2**, 1268–71.
12. O.C. Farokhzad, J. Cheng, B.A. Teply, I. Sherifi, S. Jon, P.W. Kantoff, et al, *Proc Natl Acad Sci U S A* 2006,**103**, 6315.
13. Y. Li, Y. Pei, X. Zhang, Z. Gu, Z. Zhou, W. Yuan, et al, *J Control Release* 2001, **71**, 203.
14. L. Zhang, J.M. Chan, F.X. Gu, J.W. Rhee, A.Z. Wang, A.F. Radovic-Moreno, et al, *ACS Nano* 2008, **2**, 1696.
15. J. Thevenot, A.L. Troutier, L. David, T. Delair, C. Ladaviere, *Biomacromolecules* 2007, **8**, 3651.
16. H. Shmeeda, D. Tzemach, L. Mak, A. Gabizon, *J Control Release* 2009, **136**,155.

RSC Advances Accepted Manuscript

17. W. Punfa, S. Suzuki, P. Pitchakarn, S. Yodkeeree, T. Naiki, S. Takahashi, P. Limtrakul, *Asian Pac J Cancer Prev*. 2014, 15, 9249.

18. S. Mazzucchelli, M. Truffi, L. Fiandra, L. Sorrentino, F. Corsi, *World J Pharmacol* 2014, **3**, 72.

19. M. Arruebo, M. Valladares, Á. González-Fernández, *J. Nanomaterials* 2009, Article ID 439389.

20. J.L. Arias, J.D. Unciti-Broceta, J. Maceira et al, *J Control Release*. 2015, 197, 190

21. E. Koren, A. Apte, A. Jani, V.P. Torchilin, *J Control Release* 2012, **160**, 264.

22. D. Paolino, M. Licciardi, C. Celia, G. Giammona, M. Fresta, G. Cavallaro, *Eur J Pharm Biopharm* 2012, **82**, 94.

23. D. Paolino, D. Cosco, R. Molinaro, C. Celia, M. Fresta, *Drug Discov Today* 2011,**16**, 311.

24. C. Celia, D. Cosco, D. Paolino, M. Fresta, *Med Res Rev* 2011, **31**, 716.

25. M. Celano, M.G. Calvagno, S. Bulotta, D. Paolino, F. Arturi, D. Rotiroti et al, *BMC Cancer* 2004, **4**, 63.

26. C. Celia, M.G. Calvagno, D. Paolino, S. Bulotta, C.A. Ventura, D. Russo et al, *J Nanosci Nanotechnol* 2008, **8**, 2102.

27. V.P. Torchilin, *Nat Rev Drug Discov* 2005, **4**, 145.

28. H. Wu, L. Zhu, V.P. Torchilin, Biomaterials 2013, **34**, 1213–1222.

RSC Advances Accepted Manuscript

Figure captions

Figure 1: Schematic presentation of preparation of cisplatin-loaded polymer-lipid hybrid nanoparticles. Schematic illustration shows that polymer and lipid self-assemble to form the polymer-lipid NP which was then reduced with DTT to expose the free –SH group on the surface. TSH was then conjugated with the free –SH group on the surface of nanoparticles. The core is comprised of hydrophobic PLGA core while the shell is consist of lipid materials.

Figure 2: (a) Size distribution of TSH-conjugated polymer-lipid nanoparticles (b) representative morphology characteristic of TPLHC observed by transmission electron microscopy (TEM).

Figure 3: In vitro release profile of PLHC and TPLHC formulation in phosphate buffered saline (PBS, pH 7.4) at 37°C. The release study was carried up to 48h.

Figure 4: Evaluation of selectivity of TSH-conjugated nanoparticles over non-conjugated nanoparticles. The cellular uptake was studied in chinese hamster ovary (CHO) cells without (CHO-w) (a) and with (CHO-t) the TSHr (b). Competitive binding effect of TSH-conjugated and non-conjugated nanoparticle in the presence of free TSH.

Figure 5: (a) Intracellular uptake of CDDP loaded PLHC and TPLHC formulation in FTC-133 thyroid cancer cells. (b) Confocal laser scanning microscopy images of PPLHC and TPLHC in cancer cells. In vitro cytotoxicity profile of different formulations in FTC-133 cancer cells after incubation of 24, and 48h (c-d). The cytotoxicity assay was evaluated by means of MTT assay.

RSC Advances Accepted Manuscript

Figure 6: (a-c) In vivo biodistribution of TSH-conjugated and non-conjugated nanoparticles in Wistar rats. The formulations were administered through tail vein injection and different organs were collected at specified time points.

Figure 7: Tumor suppression at the whole-body level. (a) Changes of tumor volume after intravenous injection of different formulations in tumor xenograft animal model. (b) Body weight of mice after treatments. (c) Photographs of tumor sections.

RSC Advances Accepted Manuscript

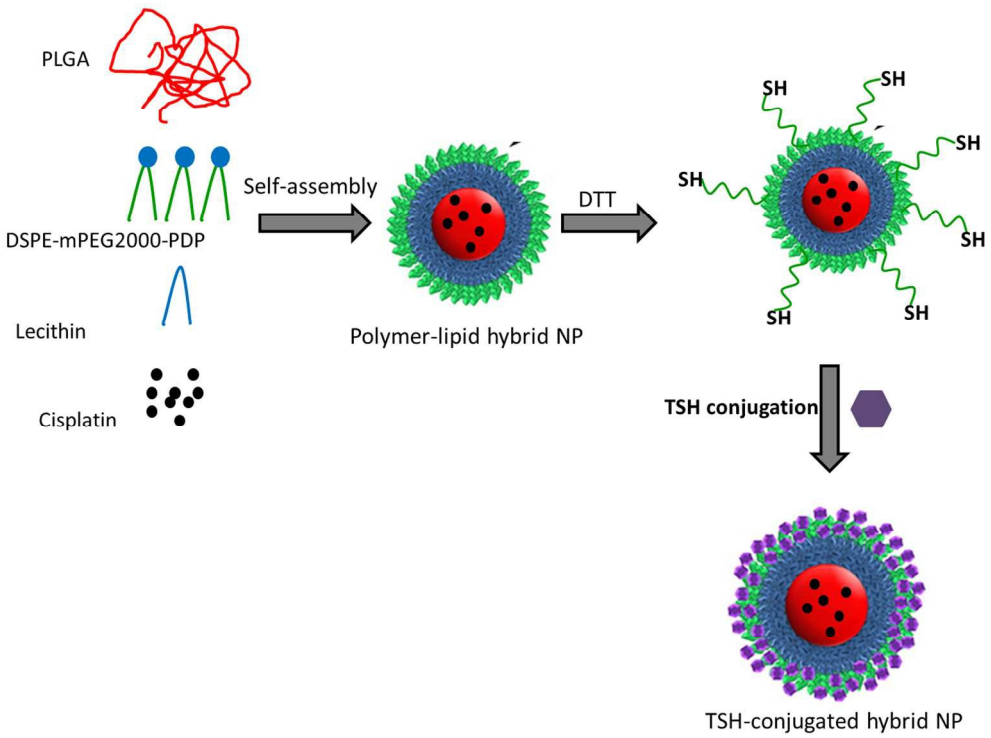

Figure 1
231x170mm (300 x 300 DPI)

RSC Advances Accepted Manuscript

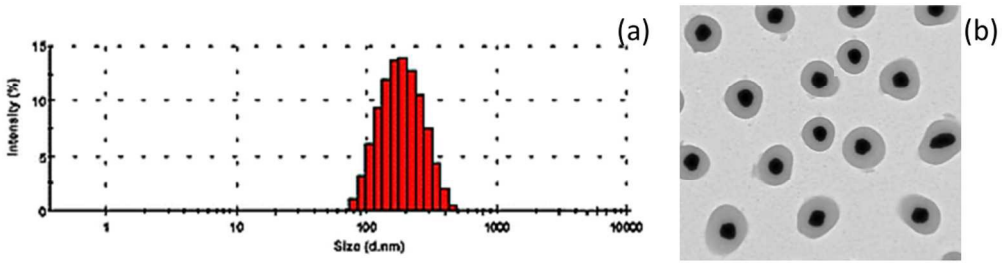

Figure 2
207x58mm (300 x 300 DPI)

RSC Advances Accepted Manuscript

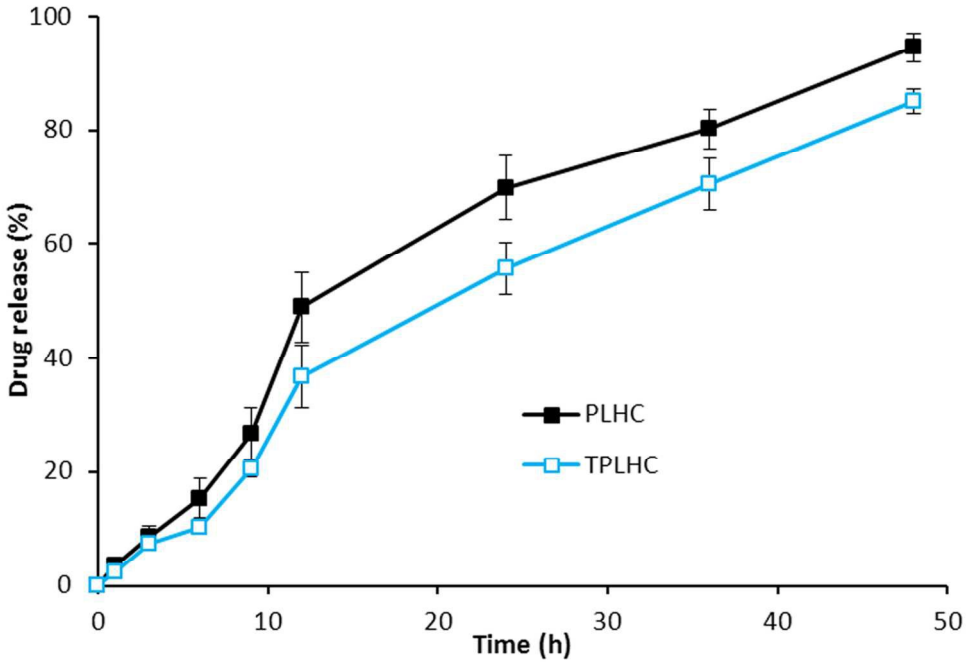

Figure 3
124x88mm (300 x 300 DPI)

RSC Advances Accepted Manuscript

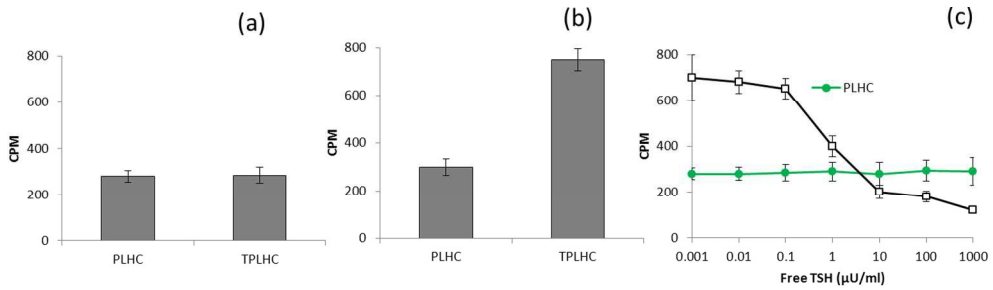

Figure 4
245x69mm (300 x 300 DPI)

RSC Advances Accepted Manuscript

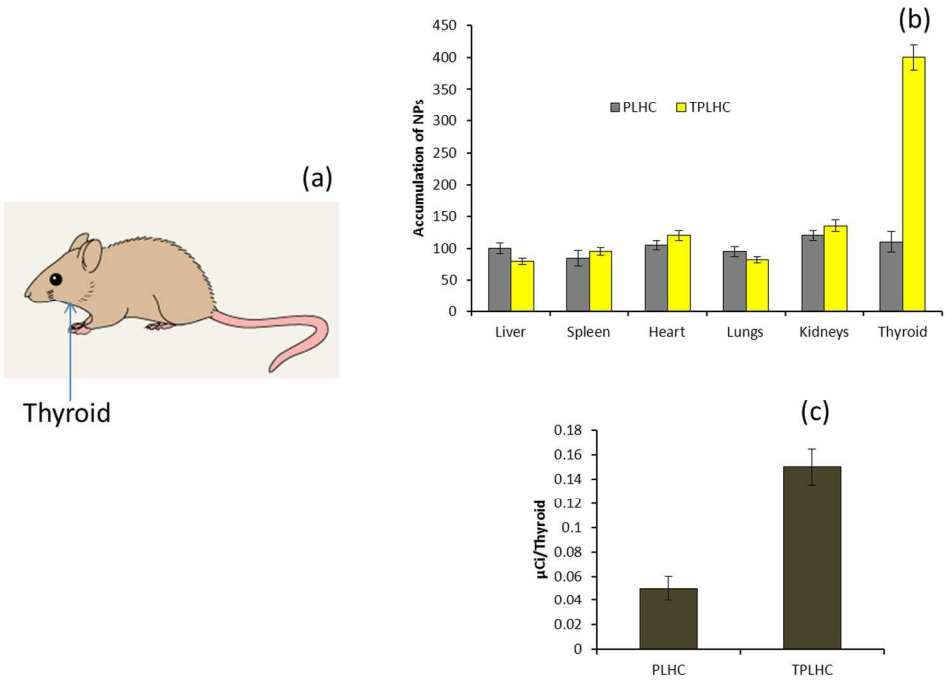

Figure 5
221x153mm (300 x 300 DPI)

RSC Advances Accepted Manuscript

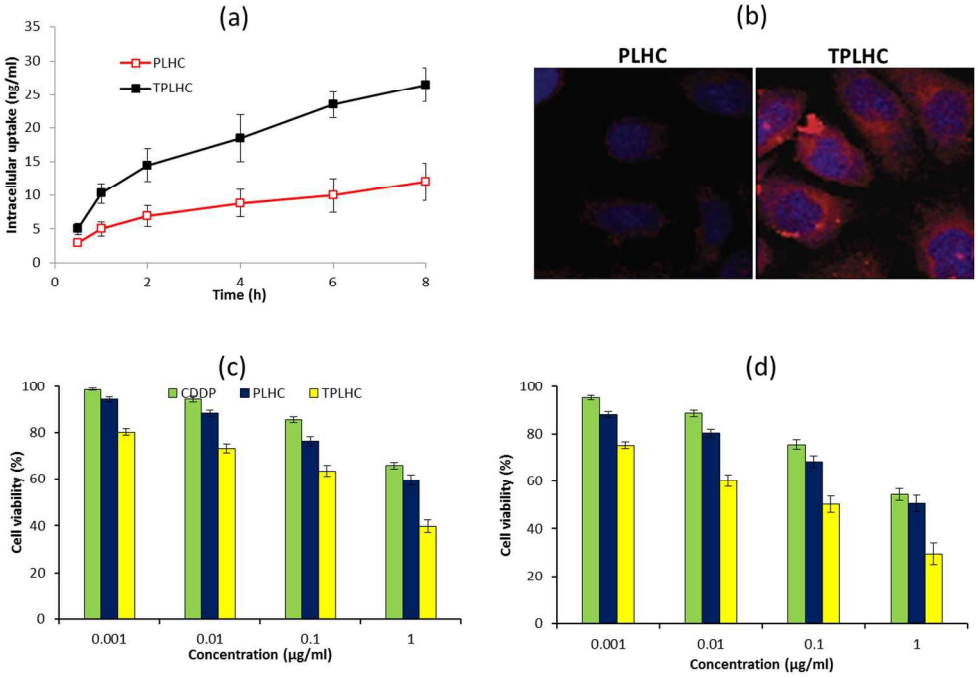

Figure 6
229x156mm (300 x 300 DPI)

RSC Advances Accepted Manuscript

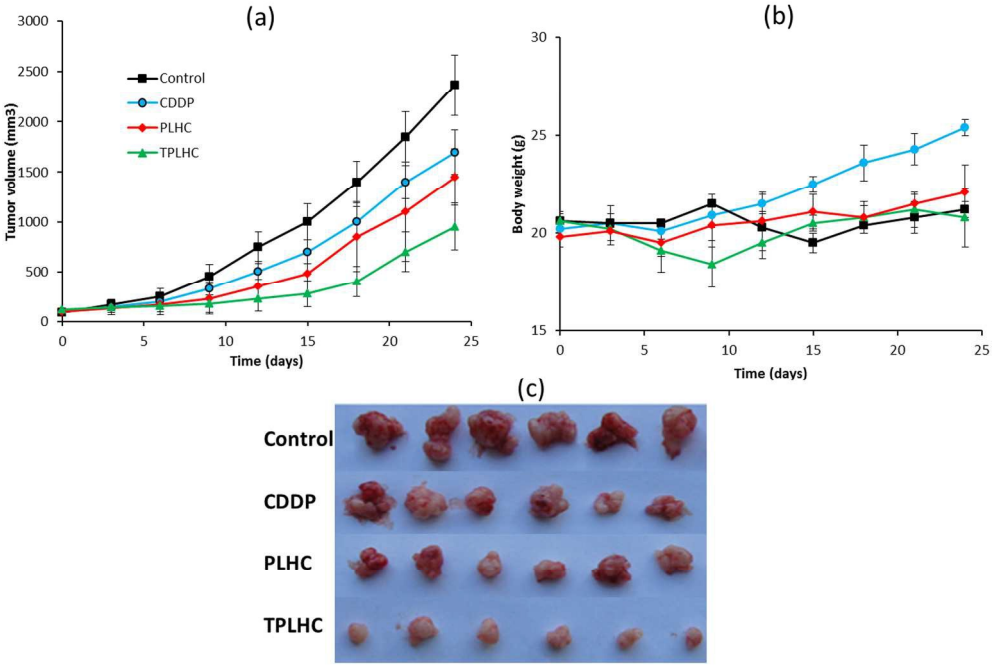

Figure 7
233x156mm (300 x 300 DPI)

RSC Advances Accepted Manuscript

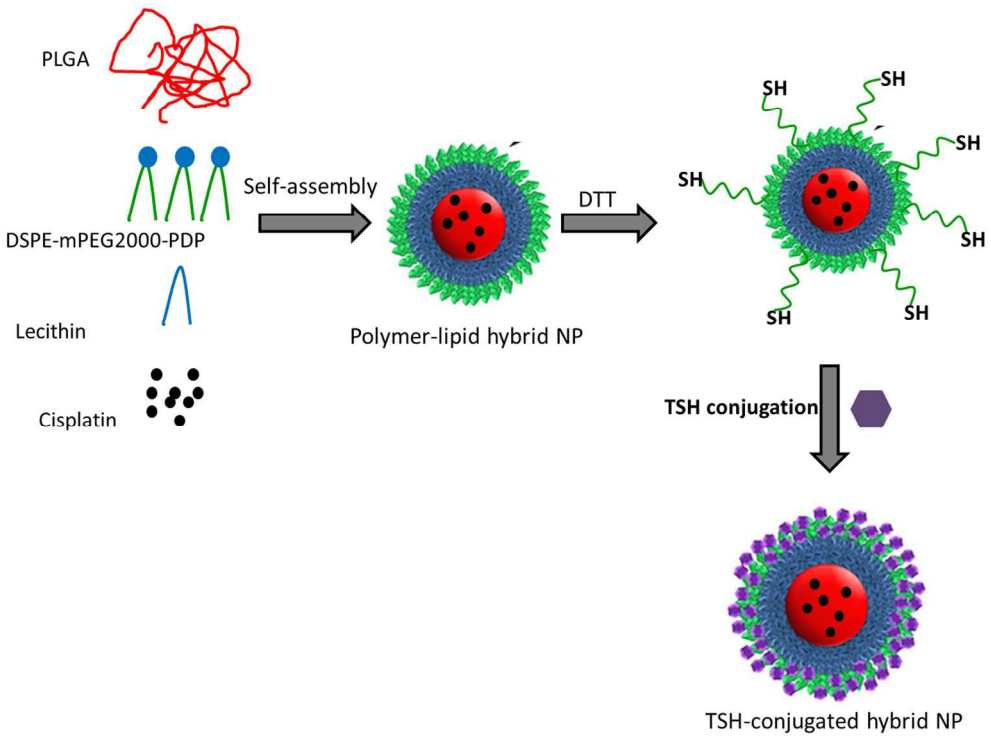

231x170mm (300 x 300 DPI)

RSC Advances Accepted Manuscript